Journal of Theoretical and Computational Chemistry
Vol. 4, Special Issue (2005) 603–622

World Scientific
www.worldscientific.com

COUPLED-CLUSTER EQUATION OF MOTION STUDY FOR THE ELECTRONIC AND OPTICAL PROPERTIES OF CONJUGATED SYSTEMS*

ZHIGANG SHUAI†, QINGXU LI and YUANPING YI

Laboratory of Organic Solids, Center for Molecular Sciences
Institute of Chemistry, Chinese Academy of Sciences
100080 Beijing, P. R. China
†*zgshuai@iccas.ac.cn*

Received 5 October 2004
Accepted 27 October 2004

We have implemented the Coupled-Cluster Equation of Motion (CC-EOM) with single and double excitations coupled with semiempirical parameterizations, Pariser–Parr–Pople model and INDO Hamiltonians, to investigate the optical and nonlinear optical properties, electronic structures and the excited states properties for the conjugated polymers. The semiempirical parameters allow us to study the conjugated systems with extensive sizes. Firstly, by comparing with the quasi-exact Density Matrix Renormalization Group theory for the 1D conjugated chain, we find that the CC-EOM approach can give satisfactory results for both the ground state and the excited states energies. We demonstrate that our approach can be adopted to evaluate linear and nonlinear response. We find that both the real and imaginary parts of the third-order polarizability can be solved either for static and dynamic responses. Then we apply the CC-EOM approach to study the optical signatures for the polarons in conjugated polymers. We have established a solid relationship between the rigidity of a polymer and its optical signature of the polarons.

Keywords: Conjugated polymer; excited states; coupled-cluster method; organic nonlinear optics; polaron; lattice relaxation.

1. Introduction

Since the pioneering discovery of conducting polymers by Alan Heeger, Alan MacDiarmid, and Hideki Shirakawa,[1] the research in this new kind of materials has become one of the most intense focus both in academia and in industry. Many fascinating applications in electrical, mechanical, optical, electronic, opto-electronic areas have been widely explored. Conducting polymers offer the promise of achieving a new generation of material, which exhibit the electrical properties of metals or semiconductors and retain the attractive mechanical properties and processing advantages of polymers.[2] They also provide an opportunity to address fundamental

*Review work dedicated to Prof. Ruozhuang Liu in the occasion to celebrate his 80th anniversary.

questions both in theoretical chemistry and in low-dimensional condensed matter physics, namely, the bond-length alternation for infinitely long one-dimensional chain,[3] the elementary excitations and topology,[4] metal-insulator transition and Peierls instability,[5] correlated low-dimensional electrons,[6] competition of electron–electron interaction and electron-phonon interaction,[7] etc.

From theoretical and computational chemistry perspectives, conducting polymers provide challenges and opportunities: the complexity of system, and the rich and novel properties. Earlier theoretical studies have played important role in understanding the doping mechanism,[8] the electronic structures,[9] and design of novel conducting polymers,[10] which had been mostly based on one-electron model. More elaborate descriptions should properly include the electron–electron correlation effects.[11] These effects are important in understanding the opto-electronic properties. It should be pointed out that recent progresses in Density-Functional-Theory (DFT) is providing a powerful tool for investigating the conducting polymers, which is out of the scope of this review. Instead, here we focus on discussing the excited states related electronic structures and optical and opto-electronic properties for the conjugated polymers.

The excited state structures constitute of a challenge for theoretical and computational chemistry. There were many studies carried out within the framework of configuration interaction (CI) with single excitations or plus double excitations. CI in general is not size-consistent, thus an extended application to large system is not allowed. CASSCF or CASPT2 has been found to be quite accurate in calculating the low-lying excited states structures for small molecules,[12] but quite time-consuming for relatively large molecules. An alternative way is the time-dependent approach, based on either the Hartree–Fock or DFT ground state,[13] which is equivalent to the Random Phase Approximation (RPA) for the two-particle Green's function. The RPA method is very efficient, and recently, a linear scaling approach has even been established for the excited states.[14] Due to the single-particle excitation character of the approach, it encounters difficulties in addressing more general excited states, especially for states with covalent nature.[15]

In this review, we present our implementation of the coupled-cluster single and double excitation equation of motion (CCSD-EOM) method and its application in both electronic structures and optical properties in conjugated systems. The model Hamiltonians here are Pariser–Parr–Pople model and semiempirical INDO Hamiltonian, which are most suitable to describe the electronic states, the optical and the nonlinear optical properties in conjugated polymer systems. Firstly, we will show that this method is highly accurate when comparing with the quasi-exact density matrix renormalization group (DMRG) theory.[16] Secondly, we present a response formalism of CCSD-EOM for the linear and nonlinear optical properties, which can give numerically converged solutions for both the real part and the imaginary part of the nonlinear susceptibility.[17] Thirdly, we apply this method to investigate the optical signature of a polaron in conjugated polymers. We have established an interesting and practical correspondence

between the rigidity of the materials and the optical absorption feature of a polaron.[18]

2. Formalism

The coupled-cluster single and double excitation (CCSD) equation of motion (EOM) approach has been shown to be accurate, efficient and size-consistent both for the molecular ground state and low-lying excited states.[19] It can calculate the ground state, excited states, and the charged states in a single unified frame.

The general electronic Hamiltonian in second quantization form reads:

$$H = \sum_{pq} h_{pq} p^+ q + \frac{1}{4} \sum_{pqrs} \langle pq| \, |rs\rangle \, p^+ q^+ sr. \tag{1}$$

Hereafter, we adopt the following convention: indices $i, j, k, l, \ldots$ refer to occupied molecular orbitals (MOs); $a, b, c, d, \ldots$ to virtual MOs and $p, q, r, s, \ldots$ generic MOs. The two-electron part is given in antisymmetric form: $\langle pq||rs\rangle = \langle pq|rs\rangle - \langle pq|sr\rangle$ and the two-electron integral is defined as:

$$\langle pq|rs\rangle = \iint dr_1 \, dr_2 \varphi_p^*(r_1) \varphi_q^*(r_2) \frac{1}{r_{12}} \varphi_r(r_1) \varphi_s(r_2),$$

with φ denoting the molecular orbital (MO) wavefunction.

2.1. *Ground state*

The CCSD ground state ansatz has been proposed as

$$|CC\rangle = \exp(T) \, |HF\rangle \, , \tag{2}$$

where $|\mathrm{HF}\rangle$ is the Hartree–Fock ground-state Slater determinant, also denoted as $|0\rangle$; and T consists of single and double excitations $T = T_1 + T_2 = \sum_{ia} t_i^a a^+ i + \sum_{\substack{i>j \\ a>b}} t_{ij}^{ab} a^+ i b^+ j$, with t's being the amplitudes of the excitation configurations. The exponential ansatz by nature guarantees the size-consistency. The ground-state energy and the excitation amplitudes are determined by the Schrödinger equation:

$$\begin{aligned} H \, |\Psi\rangle &= E_{CC} \, |\Psi\rangle \, , \quad \text{and} \\ H \exp(T) \, |0\rangle &= E_{CC} \exp(T) \, |0\rangle \, . \end{aligned} \tag{3}$$

Multiplying the above equation by $\langle 0|$, we obtain the CCSD energy expression:

$$E_{CC} = \langle 0| \, H \exp(T) \, |0\rangle = E_{HF} + \sum_{\substack{i>j \\ a>b}} \langle ij| \, |ab\rangle \left(t_{ij}^{ab} + t_i^a t_j^b - t_i^b t_j^a \right). \tag{4}$$

Multiplying Eq. (3) by $\langle 0|i^+ a$ and $\langle 0|j^+ b i^+ a$ consecutively, we obtain two nonlinear equations through which the t-amplitudes can be solved iteratively,

$$\left\langle i^+ a (H - E_{CC})(1 + T + T^2/2 + T^3/6) \right\rangle = 0, \quad \text{and} \tag{5}$$

$$\left\langle j^+ b i^+ a (H - E_{CC})(1 + T + T^2/2 + T^3/6 + T^4/24) \right\rangle = 0. \tag{6}$$

The natural choice of the initial solution is:

$$t_i^a = 0, \quad t_{ij}^{ab} = \frac{\langle ij|\,|ab\rangle}{\varepsilon_i + \varepsilon_j - \varepsilon_a - \varepsilon_b}. \tag{7}$$

Substituting the initial solution Eq. (7) into Eq. (4), it is seen that the energy corresponds exactly to the MP2 approximation.

2.2. *Excited states*

Based on the CCSD ground state, we can establish the Heisenberg equation of motion in the Hilbert subspace constructed by promoting one and two electrons from occupied to virtual MOs. We denote the excitation operators as μ, ν, σ, etc. The excited-state wavefuntion is constructed as a linear combination of all the single and double excitations on the CCSD ground state:

$$|ex\rangle = \sum_\mu R_\mu \exp(T)\,|\mu\rangle\,, \tag{8}$$

where $|\mu\rangle = \mu|HF\rangle$ represents an excitation determinant and R_μ is the corresponding coefficient to be determined. The excited-state Schrödinger equation becomes

$$H\,|ex\rangle = E\,|ex\rangle\,; \quad H\sum_v R_\nu \exp(T)\,|\nu\rangle = E\sum_\nu R_\nu \exp(T)\,|\nu\rangle, \tag{9}$$

where E is the excited state energy. When multiplying the above equation by $\exp(-T)$ from the left and then multiplying an excitation ket configuration $\langle\mu|$, we obtain the following eigen-equation:

$$\sum_\nu \bar{H}_{\mu\nu} R_\nu = E R_\mu, \tag{10}$$

where

$$\begin{aligned}\bar{H} &= \exp(-T) H \exp(T) \\ &= H + [H,T] + \frac{1}{2}[[H,T],T] + \frac{1}{6}[[[H,T],T],T] \\ &\quad + \frac{1}{24}[[[[H,T],T],T],T]\end{aligned} \tag{11}$$

is the similarity transformed Hamiltonian. The expansion terminates exactly after 5 terms, because the two-electron term of the Hamiltonian consists of 4 generic Fermion operator and each commutation with the excitation operator eliminates one generic index, thus in the last term of Eq. (11), there is no more generic index and it commutes with any excitation operator. In fact, in all the mathematics manipulations, the fact that all the excitation operators commute has been widely employed. We give the full expression of Eq. (11) in Appendix.

We can extract the ground state energy E_{CC} from the excited state:

$$E = E_{CC} + \Delta E_{ex}. \tag{12}$$

Multiplying $\exp(-T)$ from left to Eq. (3), we have $\bar{H}|0\rangle = E_{CC}|0\rangle$. Then, we can recast the Eq. (10) as:

$$\sum_{\nu} \left\{ \langle \nu|\bar{H}|\mu\rangle R_\nu - E_{cc}\langle \nu|\mu\rangle R_\nu \right\} = R_\mu \Delta E$$

or

$$\sum_{\nu} R_\nu \langle \nu|[\bar{H},\mu]|0\rangle = R_\mu \Delta E. \tag{13}$$

This is the Heisenberg equation of motion for the effective Hamiltonian. The similarity transformed Hamiltonian is no longer Hermitian, or under the real basis, its matrix representation is no longer symmetric. Then, corresponding to each eigenvalue, there exist a right eigenvector and a left eigenvector. The left eigenvector is expressed as:

$$\langle ex| = \sum_{\mu_1} \langle \mu|L_\mu \exp(-T). \tag{14}$$

L_μ can be determined in a similar way as for R_μ.

In order to evaluate the physically measurable quantity, we also need the left eigenvector of the CCSD ground state, i.e. the so-called Λ state in the CCSD gradient theory,[20] which is defined as

$$\langle L_0| = \langle 0|(1+\Lambda)\exp(-T),$$

where $\Lambda = \sum_{ia} \lambda_a^i i^+ a + \sum_{\substack{i>j \\ a>b}} \lambda_{ab}^{ij} i^+ a j^+ b$ is the de-excitation operator.

Note that $\langle L_0|CC\rangle = 1$. The coefficient λ's are determined by the Schrödinger equation for $\langle L_0|$:

$$\langle L_0|H = \langle 0|(1+\Lambda)\exp(-T)H = \langle 0|(1+\Lambda)\exp(-T)E_{CC}.$$

Multiplying $\exp(T)\ \eta|0\rangle$ to the right of the above equation, we can obtain the following linear equation:

$$\sum_{\nu} \lambda_\nu A_{\nu\mu} = -\langle 0|\bar{H}|\mu\rangle. \tag{15}$$

From which the Λ amplitudes can be solved for given T amplitudes. This left ground state is essential for evaluating the physically measurable quantities, for instance, the optical transition and nonlinear responses.

2.3. *Positively charged states*

When an electron is ionized from a polymer chain, its eigenstates within the CCSD-EOM approach can be constructed in the excitation space $|\sigma\rangle = \{n, g^+ no\}$, where indices n, o refer to occupied MOs and g refer to virtual MOs. Then the

eigenstates are

$$|p\rangle = \sum_{\sigma} X_\sigma \exp(T)\,|\sigma\rangle\,, \quad \text{and} \tag{16}$$

$$\langle p| = \sum_{\sigma} \langle\sigma|Y_\sigma \exp(-T). \tag{17}$$

To derive the eigen-equation, we insert Eq. (8) to the Schrödinger equation, and take the coupled cluster ground state energy as the zero point for energy,

$$(H - E_{cc})\,|p\rangle = (E - E_{cc})\,|p\rangle\,, \tag{18}$$

which yields

$$(H - E_{cc}) \sum_{\sigma} X_\sigma \exp(T)\,|\sigma\rangle = (E - E_{cc}) \sum_{\sigma} X_\sigma \exp(T)\,|\sigma\rangle\,. \tag{19}$$

When multiplying the above equation by $\exp(-T)$ from the left and then multiplying $\langle\sigma|$, we obtain the following eigen-equation:

$$\sum_{\rho} (\bar{H}_{\sigma\rho} - E_{CC}\delta_{\sigma\rho})X_\rho = \Delta E X_\sigma, \tag{20}$$

where $\Delta E = E - E_{CC}$ is the ionization potential (IP).

Similarly, we can obtain the eigen-equation about Y_σ

$$\sum_{\sigma} Y_\sigma(\bar{H}_{\sigma\rho} - E_{CC}\delta_{\sigma\rho}) = \Delta E Y_\rho. \tag{21}$$

Within the single and double excitation space, for $S_z = 1/2$, there are six microstates, which can be linearly combined to form the spin adapted basis. There are two vectors for $S = 3/2$, which we do not consider in this work, and four vectors for $S = 1/2$:

$$\text{(i)}\quad |m_\beta\rangle\,, \tag{22a}$$

$$\text{(ii)}\quad \left|c_\alpha^+ m_\alpha m_\beta\right\rangle, \tag{22b}$$

$$\text{(iii)}\quad \left(2\left|c_\beta^+ m_\beta l_\beta\right\rangle + \left|c_\alpha^+ m_\alpha l_\beta\right\rangle + \left|c_\alpha^+ m_\beta l_\alpha\right\rangle\right)/\sqrt{6} \quad (\text{with } m > l), \tag{22c}$$

$$\text{(iv)}\quad \left(\left|c_\alpha^+ m_\alpha l_\beta\right\rangle - \left|c_\alpha^+ m_\beta l_\alpha\right\rangle\right)/\sqrt{2} \quad (\text{with } m > l). \tag{22d}$$

The $S_z = -1/2$ spin eigenstates $|\sigma\rangle_\downarrow$ is obtained by exchanging the indices α and β of eigenstates $|\sigma\rangle_\uparrow$.

2.4. *Negatively charged states*

When attaching an electron to a molecule, we obtain the eigenstates by using $|\nu\rangle = \{e^+, e^+f^+m\}$, where indices m refer to occupied MOs and e,f refer to virtual Mos.

Then the eigenstates are

$$|n\rangle = \sum_{\nu} U_{\nu} \exp(T) \, |\nu\rangle \, , \quad \text{and} \quad \langle n| = \sum_{\nu} \langle \nu | V_{\nu} \exp(-T). \tag{23}$$

Similar to the positive charge states, we can obtain then eigen-equation about U_ν and V_ν:

$$\sum_{\mu} (\bar{H}_{\mu\nu} - E_{CC}\delta_{\mu\nu}) U_{\mu} = \Delta E' U_{\nu}, \quad \text{and} \tag{24}$$

$$\sum_{\nu} V_{\mu} (\bar{H}_{\mu\nu} - E_{CC}\delta_{\mu\nu}) = \Delta E' Y_{\nu}, \tag{25}$$

where $\Delta E' = E - E_{CC}$ is electron affinity (EA).

The matrix elements for the similarity transformed Hamiltonian $\bar{H}_{\mu\nu}$ are evaluated in the same way as in the positively charged case, which we omit here.

There are four types of $S_z = 1/2$ eigenstates $|\nu\rangle_{\uparrow}$:

$$\text{(i)} \quad \left|e_{\alpha}\right\rangle, \tag{26a}$$

$$\text{(ii)} \quad \left|e_{\alpha}^{+} e_{\beta}^{+} k_{\beta}\right\rangle, \tag{26b}$$

$$\text{(iii)} \quad \left(2\left|e_{\alpha}^{+} d_{\alpha} k_{\alpha}\right\rangle + \left|e_{\alpha}^{+} d_{\beta} k_{\beta}\right\rangle + \left|e_{\beta}^{+} d_{\alpha} k_{\beta}\right\rangle\right)/\sqrt{6} (d > e), \tag{26c}$$

$$\text{(iv)} \quad \left(\left|e_{\alpha}^{+} d_{\beta}^{+} k_{\beta}\right\rangle - \left|e_{\beta}^{+} d_{\alpha} k_{\beta}\right\rangle\right)/\sqrt{2} (d > e). \tag{26d}$$

The $S_z = -1/2$ spin eigenstates $|\nu\rangle_{\downarrow}$ is obtained by exchanging the indices α and β of eigenstates $|\nu\rangle_{\uparrow}$.

To verify the accuracy of our implementation of EOM-CCSD, we have made a comparison with the density matrix renormalization group (DMRG) calculation on a pi-electron Pariser–Parr–Pople model with long-range Coulomb interaction of Ohno–Klopman potential. The Hamiltonian reads:

$$H = -\sum_{\langle \mu\nu \rangle s} t_{\mu\nu} (c_{\mu,s}^{+} c_{\nu,s} + \text{h.c.}) + U \sum_{\mu} n_{\mu\uparrow} n_{\mu\downarrow} + \sum_{\mu<\nu} V(r_{\mu\nu}) (n_{\mu} - 1)(n_{\nu} - 1), \tag{27}$$

where t is the pi-electron hopping integral, U is the on-site Hubbard term, and V is the long-range density–density interaction. The parameters for hydrocarbon bond are chosen as: $U = 11.13\,\text{eV}, t(\text{double bond}) = -2.6\,\text{eV}, t(\text{single bond}) = -2.2\,\text{eV}, t(\text{phenyl-ring-bond}) = -2.4\,\text{eV}$. For a polyene chain with 20 pi-electrons, the ground state energy as well as a few optically important excited state energies is computed within a symmetrized DMRG with ling range interaction and the EOM-CCSD, and are listed for comparison in Table 1.

The $1B_u$ state corresponds to the lowest-lying and (optically) most active exciton state with a large oscillator strength. The $2A_g$ state is the lowest-lying even-parity exciton state, which has been described by Tavan and Schulten as a combination of two triplet excitations.[15] In the strong correlation regime where charge and spin degrees of freedom can be separated, $1B_u$ is a charge excitation and $2A_g$ a spin excitation. In the weak correlation limit, a simple molecular orbital promotion picture is applied to represent the excited state. Then, the $2A_g$ state lies

Table 1. Comparison of the state energies (in eV) of linear polyenes with 20 sites calculated at the CCSD-EOM and SDMRG levels. The excited state energies are given relative to the ground state. The Hartree-Fock $1A_g$ ground state energy is -40.7979 eV, and the MP2 energy is -42.0602 eV.

	$1A_g$	$1B_u$	$2A_g$	mA_g	nB_u1	nB_u2
DMRG	−43.73175	3.450	2.727	5.422	7.205	5.439
CC-EOM	−43.60039	3.360	3.270	5.415	7.830	5.715

above the $1B_u$ state. The fact that both SDMRG and EOM-CCSD give $2A_g$ below $1B_u$ manifests the importance of electron correlation, is in good agreement with the experiments.[11] An upper-lying even-parity state, the mA_g state is characterized by a large transition dipole moment with the $1B_u$ state, which has been shown to be an even-parity ionic excited state.[21]

Note that for this model Hamiltonian, the DMRG results can be regarded as nearly exact.[22] From Table 1, we see that the EOM-CCSD results agree very well with the DMRG, though only the $2A_g$ state demonstrates the largest deviation, but the relative ordering with respect to $1B_u$ is correct.

3. Linear and Nonlinear Optical Responses

Under the electric dipole approximation, the interaction between molecule and a radiation field can be described by the electric dipole operator:

$$\hat{O} = -e\sum_i \vec{r}_i + \sum_A Z_A \vec{R}_A, \tag{28}$$

where r_i is the position operator for electron, and R_A is the position of atomic nuclear, which is taken as a c-number here. The one-electron operator $\hat{O}$ can be expressed in second quantization:

$$\hat{O} = \sum_{pq} O_{pq} p^+ q, \tag{29}$$

where $O_{pq} = \int \psi_p^*(1) O(1) \psi_q d1$, which is obtained within the Hartree–Fock MO solutions.

Consider a general evaluation of electric dipole transition between two states,

$$\langle m|\hat{O}|n\rangle = \sum_{\mu\nu} L_\mu^m R_\nu^n \langle \mu| \exp(-T)\hat{O}\exp(T)|\nu\rangle. \tag{30}$$

Thus, the dipole operator should also be Hausdorff-transformed.

Linear and nonlinear optical responses can be formally expressed as sum-over-states (SOS) approaches, here, we refer the reader to Orr and Ward's classical work,[23] which we omitted here. The SOS approach has played a central role in understanding the linear and nonlinear optical spectra, as well as the microscopic mechanism and structure-properties relationship. Apart from the SOS approach, the finite-field or couple-perturbed methods have been widely implemented in the quantum chemical packages, which in general can give static and sometimes

dynamic optical susceptibility values. But as far as the spectra and the physical origins are concerned, the SOS approach is more practical. In many cases, summing over all states is impractical. An alternative method, which can avoid the summation over all states, and in principle, the dynamical responses can be evaluated. Here, we briefly introduce our implementation of this latter approach, the so-called correction vector method within the context of EOM-CCSD. We refer the details of this implementation to Shuai and Brédas,[17] and Shuai *et al.*[24]

Define two operators F and G:

$$F_{\mu\nu} = A_{\mu\nu} - (\hbar\omega + i\Gamma)\delta_{\mu\nu}; \quad G_{\mu\nu} = A_{\mu\nu} + (\hbar\omega + i\Gamma)\delta_{\mu\nu}, \tag{31}$$

where matrix A is the Jacobian: $A_{\mu\nu} = \bar{H}_{\mu\nu} - E_{CC}\delta_{\mu\nu}$, ω is the frequency of incident light, and Γ is an empirical damping factor. By solving the following two linear equations:

$$\sum_{\nu} F_{\mu\nu}\phi^i_\nu(-\omega) = \langle\mu|\,\overline{er}^i\,|0\rangle\,; \quad \sum_{\nu} G_{\mu\nu}\phi^i_\nu(\omega) = \langle\mu|\,\overline{er}^i\,|0\rangle \tag{32}$$

where superscript i is the Cartesian space coordinate index, we can obtain the vectors ϕ's, the so-called first-order correction vectors. The physical meaning of this vector is the first-order correction of the ground-state wavefunction upon time-dependent electric field perturbation. It can be easily shown that the first-order polarizability is recast from an SOS expression as:

$$\alpha^{ij}(\omega) = \sum_{\mu} \left\{ \langle 0|\,(1+\Lambda)\overline{er}^i\,|\mu\rangle\,\phi^j_\mu(-\omega) + \langle 0|\,(1+\Lambda)\overline{er}^j\,|\mu\rangle\,\phi^i_\mu(+\omega) \right\}. \tag{33}$$

Here, we have employed the fact that the eigenfunction matrix that diagonalizes the Jacobian can also diagonalize the inverse matrices of F and G: F and G are nothing but Jacobian plus a diagonal constant term. Similarly, we can obtain the expression for β, the second-order polarizability:

$$\begin{aligned}\beta^{ijk}(\omega_1,\omega_2) = I_{1,2}\sum_{\mu} \langle 0|\,(1+\Lambda)\,\{\overline{er}^i\,|\mu\rangle\,\psi^{kj}_\mu(-\omega_1-\omega_2,-\omega_1) \\ + \overline{er}^k\,|\mu\rangle\,\psi^{ji}_\mu(\omega_2,\omega_1+\omega_2) + \overline{er}^j\,|\mu\rangle\,\psi^{ik}_\mu(\omega_1,-\omega_2)\}.\end{aligned} \tag{34}$$

$I_{1,2}$ represents a summation over permutations of (ω_1, j) with (ω_2, k). The second-order correction vector ψ is solved by the following linear equation:

$$\sum_{\nu}\{A_{\mu\nu} + (\hbar\omega_1 + i\Gamma)\delta_{\mu\nu}\}\psi^{ik}_\nu(\omega_1,-\omega_2) = \sum_{\sigma}(\overline{er}^i)_{\mu\sigma}\phi^k_\sigma(-\omega_2), \quad \text{and so on.} \tag{35}$$

And for the third-order, we can obtain

$$\begin{aligned}\gamma^{ijkl}(\omega_1,\omega_2,\omega_3) = I_{123}\sum_{\nu\sigma}\{&\kappa^i_\nu(-\omega_1-\omega_2-\omega_3)(\overline{er}^l)_{\nu\sigma}\psi^{kj}_\sigma(-\omega_1-\omega_2,-\omega_1) \\ &+ \kappa^l_\nu(\omega_3)(\overline{er}^i)_{\nu\sigma}\psi^{kj}_\sigma(-\omega_1-\omega_2,-\omega_1) \\ &+ \kappa^j_\nu(\omega_1)(\overline{er}^k)_{\nu\sigma}\psi^{il}_\sigma(\omega_1+\omega_2,-\omega_3) + \kappa^j_\nu(\omega_1)(\overline{er}^k)_{\nu\sigma}\psi^{li}_\sigma(\omega_1 \\ &+ \omega_2,\omega_1+\omega_2+\omega_3)\}\end{aligned}$$

$$
\begin{aligned}
&- I_{123}\{(\rho^{il}(-\omega_1-\omega_2-\omega_3)\rho^{kj}(-\omega_1)+\rho^{li}(\omega_3)\rho^{kj}(-\omega_1))/\\
&(-\omega_1-\omega_2-i\Gamma)\\
&+(\rho^{jk}(\omega_1)\rho^{il}(-\omega_3)+\rho^{jk}(\omega_1)\rho^{li}(\omega_1+\omega_2+\omega_3))/\\
&(\omega_1+\omega_2+i\Gamma)\}, \qquad (36)
\end{aligned}
$$

where I_{123} represents a summation over permutations of $(\omega_1, j), (\omega_2, k)$, and (ω_3, l) (six of them in total). We have introduced two more quantities, the vector κ and the scalar ρ. They are defined as:

$$\sum_{\nu}\{A_{\nu\mu}+(\hbar\omega+i\Gamma)\delta_{\nu\mu}\}\kappa^i_\nu(\omega)=\langle L_0|\,(1+\Lambda)(\overline{er}^i)\,|\mu\rangle\,, \qquad (37)$$

$$\rho^{ij}(\omega)=\sum_{\mu}\langle L_0|\,(1+\Lambda)(\overline{er}^i)\,|\mu\rangle\,\phi^j_\mu(\omega). \qquad (38)$$

In fact, κ differs from ϕ only due to the non-symmetric nature of the Jacobian.

It should be noted that there occur linear equations of the form $Ax = b$ in several instances in solving the correction vectors. We apply an algorithm in fully parallel to the Davidson diagonalization scheme in solving these equations.

For a fixed chain length, $N = 30$, we have studied the dynamic linear and nonlinear response spectra, using the correction vector approach. The total excitation-dimensional is of about 150 thousand. For each incident light frequency, all the correction vector linear equations are solved. Very often, the linear equation is not stable when the frequency is approaching the resonance, because the matrix is no more positive definite. To avoid such a divergence, we have introduced a damping factor, an imaginary term, in to the linear equation, and for the negative frequency component equation, we have multiplied both sides of the equation by the transpose of the matrix, namely, we transform the $Ax = b$ to be $A^TAx = A^Tb$, which guarantee the matrix to be always positive definite. After doing all these, we find that our codes are quite stable, and the obtained linear and nonlinear spectra are depicted in Figs. 1 and 2. The imaginary part of linear polarizability corresponds to the optical absorption spectra, which convey the message of the excited state structures. Here, we emphasize that without calculating the excited states, our approach can obtain the full spectrum. The dispersion curve of the third-order polarizability for the third-harmonic generation (THG) in Fig. 2 presents rich resonance structures, which reveals the three-photon resonances and the two-photon resonances in THG processes, which has been in the center of interests. Here we will not go into the details of these structures. Instead, we stress that the EOM-CCSD-CV calculated spectra are comparable to those obtained in the SDMRG-SOS approach obtained by Shuai *et al.*, where a few hundreds of excited states have been calculated.[25] While in the present approach, we only need the ground state and the Hilbert space in which the Hausdorff-transformed Hamiltonian is expanded.

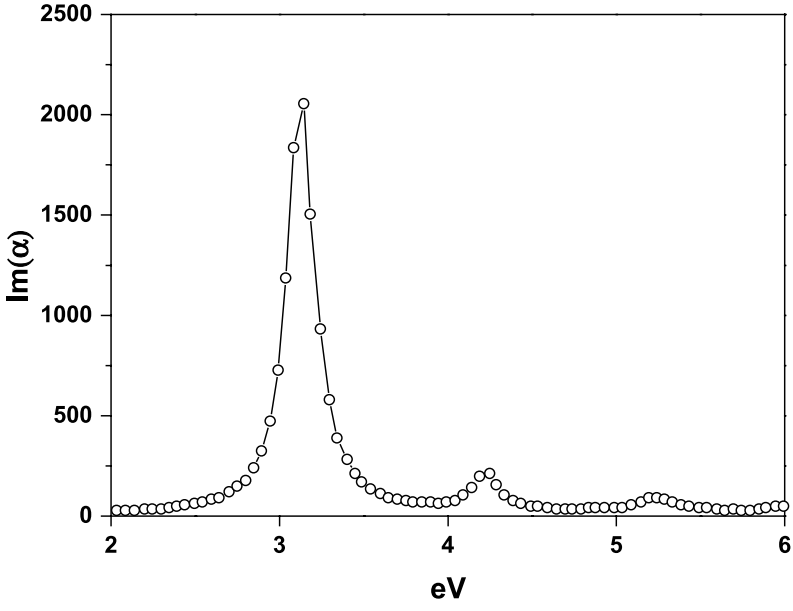

Fig. 1. Optical absorption spectrum calculated from EOM-CCSD linear response formulation, for polyne/PPP model.

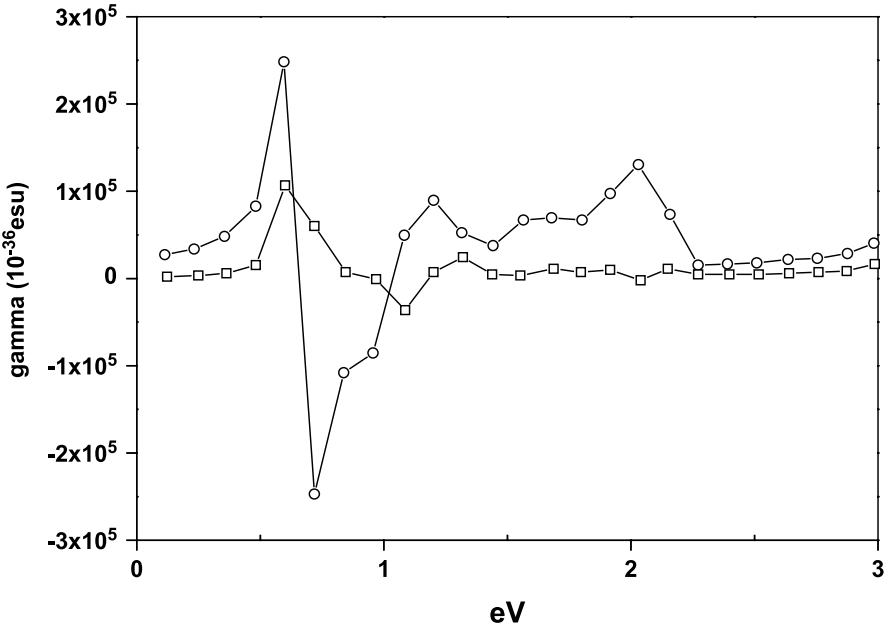

Fig. 2. Third-harmonic generation spectrum calculated through EOM-CCSD nonlinear response formulation for polyene/PPP model: open diamond for the real part, open square for the imaginary part.

4. Optical Signatures of Charged Conjugated System

The PPP model can describe well the hydrocarbon systems with much less computational efforts than the *ab initio* method. Another more general simple model is the INDO Hamiltonian. This method has been found to be very successful in describing the electronic excitations from organic molecules to transition metals with semiempirical parameters. We note that the correlation effects dominate the electronic excitation and its dynamical processes. These effects are usually responsible for the physical origins. Recently, we have also incorporated the EOM-CCSD formalism with the INDO Hamiltonian,[18,26] which give satisfactory results when comparing with high level treatment such as CASPT2. In Table 2, we make such a comparison. It is observed that the INDO-EOM-CCSD works quite well and can be extended to much larger systems than what the *ab initio* approach can afford.

Charged conjugated species play essential roles in polymer electronics and optoelectronics. In electroluminescence and field effect devices, charges are injected from electrodes. Upon addition of positive or negative charges to the conjugated chains, new electronic states are created. These charges can result from chemical or electrochemical doping. Charge injection gives rise to the appearance of spatially localized geometric defects, the polarons, as a result of the strong electron-phonon coupling that is characteristic of conjugated chains.[5,8] The formation of polarons induces major modifications in the electronic structure of the conjugated chains (see Fig. 3): two new localized one-electron levels, i.e., a lower polaron level (POL1) and an upper polaron level (POL2), appear within the original gap, as shown in Fig. 3.[28] For a singly positively (negatively) charged state, the lower (upper) polaron level is singly occupied. According to the one-electron picture, two new subgap optical transitions are expected in an oligomer: HOMO $\rightarrow$ POL1(POL2 $\rightarrow$ LUMO) and POL1 $\rightarrow$ POL2. Here, we apply coupled cluster approach to the description of the optical properties of a wide range of conjugated systems in their singly-charged state. Our goal is two-fold: (i) to address the accuracy of our approach for the calculation of polaron absorption spectra; and (ii) to explore the dependence on chemical structure of the polaron optical transition energies and intensities.

We report in this section our studies of the optical properties of polarons in oligomers of polyacetylene (PA), polythiophene (PT), polyparaphenylene (PPP), and polyparaphenylene vinylene (PPV).[18] These polymers are at the center stage for polymer electronic and optoelectronic applications.[29] The systems in computation are oligomers with increasing number of unit cells. The geometries

Table 2. Comparison of transition energies (in eV) for organic radical cations as calculated at our semiempirical INDO/EOM-CCSD, INDO/CIS, *ab initio* CASPT2, TD-DFT levels, and measurement.[27]

	INDO-EOM-CCSD	INDO-CIS	CASPT2	TD-DFT(BLYP)	Experiments
1^2A_u(ethylene$^+$)	3.01	2.64		3.26	
1^2A_u(terthiophen$^+$)	1.23	0.92	1.31	1.65	1.46
2^2A_u(terthiophene$^+$)	1.90	1.87	1.94	2.65	2.25

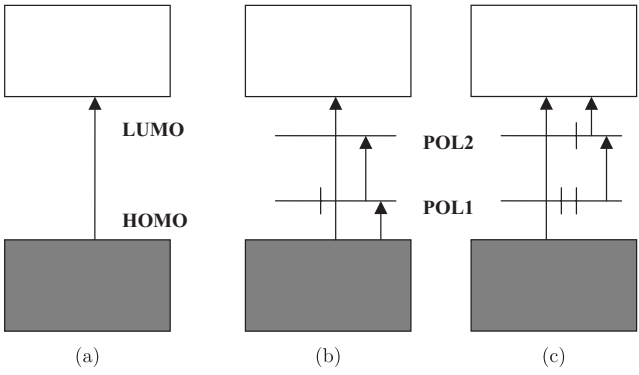

Fig. 3. Schematic one-particle representation of the optical processes in neutral (a), hole polaron (b), and electron polaron (c) states. The short vertical bars represent electron occupation.

both for neutral and charged states are fully optimized at the semiempirical Hartree–Fock semiempirical Austin Model 1 (AM 1) level. We illustrate the structural modifications of the central parts of these oligomers upon geometry relaxation due to the extra charge in Table 3.

The optical absorption spectrum is simulated by calculating the imaginary parts of the linear susceptibility:

$$I(\omega) = \omega \,\mathrm{Im}[\alpha(-\omega;\omega)]$$
$$= \omega \,\mathrm{Im}\left[\sum_{m\neq g} \frac{\langle g|\mu|m\rangle\langle m|\mu|g\rangle}{\langle m|m\rangle}\left(\frac{1}{E_m - E_g - \hbar\omega - i\Gamma} + \frac{1}{E_m - E_g + \hbar\omega + i\Gamma}\right)\right], \tag{39}$$

Table 3. AM1-optimized geometry deformations in the central part of different oligomers: $C_{20}H_{22}$, OT5, OP5, and OPV5. The C–C bond lengths in the neutral state and the positive polaron state are given in Å; Δ is the change in bond length when going from the neutral state to the polaron.

Oligomer	Central Part	Bond	Neutral State	Polaron	Δ
$C_{20}H_{22}$	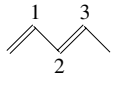	1–2	1.444	1.395	−0.049
		2–3	1.347	1.392	0.045
OT5	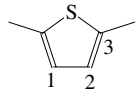	1–2	1.419	1.383	−0.036
		2–3	1.390	1.430	0.04
OP5	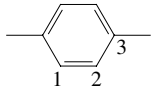	1–2	1.391	1.373	−0.018
		2–3	1.402	1.426	0.024
OPV5	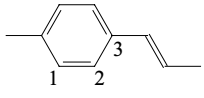	1–2	1.390	1.372	−0.018
		2–3	1.406	1.429	0.023

where $m(g)$ is the index for the excited (ground) state, ω is the frequency of incident light, μ is the electric dipole operator, and Γ is a broadening factor, which is set to be 0.05 eV in this study.

The calculated optical absorption spectra for the polaron presented in the series of oligomers with increasing lengths are depicted in Figs. (4)–(7). From these spectra, one can note that (i) there always appear two sub-gap absorption peaks, the lower energy peak (LE) and the high energy peak (HE), and (ii) the intensity for HE for long polyene and thiophene is higher than that of LE, while for long OP and OPV are in contrast. The origin of these two sub-gap peaks have been analyzed in Fig. 3, as discussed in previous paragraph. The relative intensity manifests the competition of electron–electron correlation and electron-phonon interaction. In a one-electron picture, the LE should be more pronounced than the HE. However, once electron interaction effect comes to play, the quantum interference between these optical transitions becomes important. In the EOM-CCSD framework, the electric dipole transition is expressed as:

$$\langle g\,|\mu\,|m\rangle = \sum_{\nu\sigma} L_\sigma^g R_\nu^m \left\langle \sigma\middle|e^{-T}\mu e^{T}\,|\nu\right\rangle = \sum_{\nu\sigma} L_\sigma^g R_\nu^m \bar{\mu}_{\sigma\nu}. \tag{40}$$

For the hole polaron, it is observed from the numerical calculations that (i) the ground state is dominated by removing a electron from the HOMO ($L = 0.95$), (ii) the LE and HE excited states are dominated by the HOMO → POL1 and

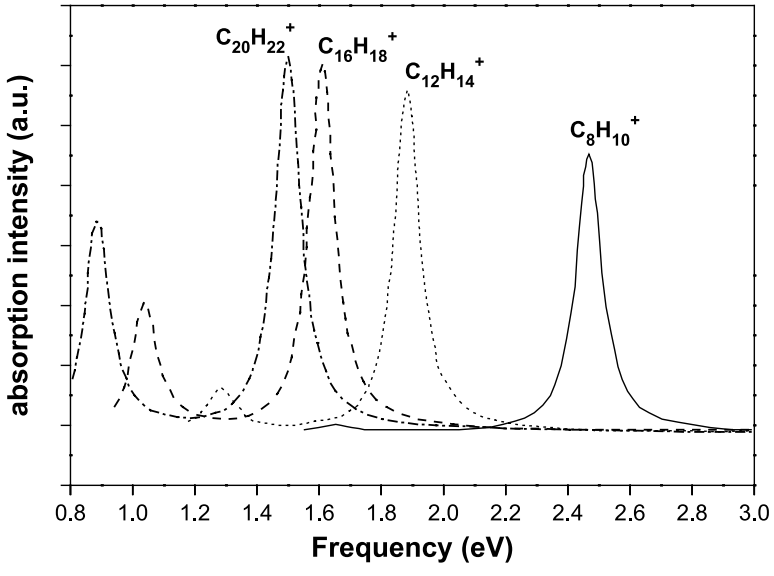

Fig. 4. EOM-CCSD/INDO calculated optical absorption spectra of hole polaron in polyenes with increasing size.

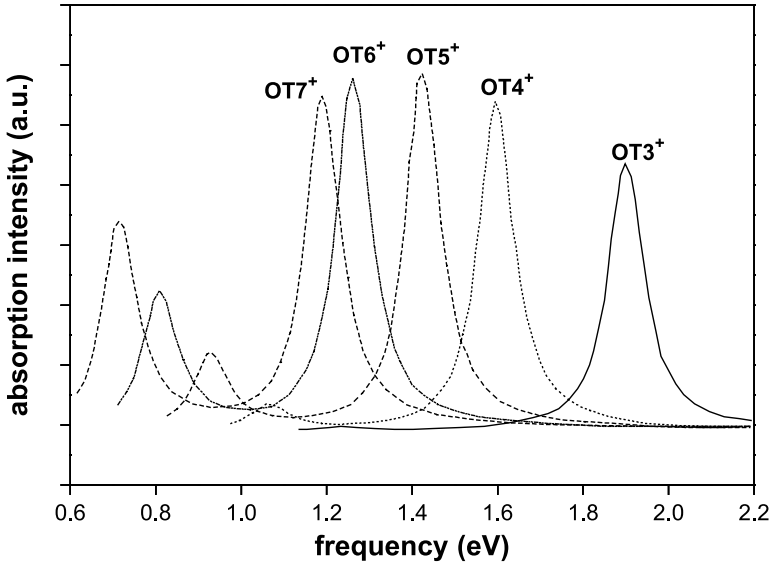

Fig. 5. EOM-CCSD/INDO calculated optical absorption spectra of hole polaron in oligothiophenes.

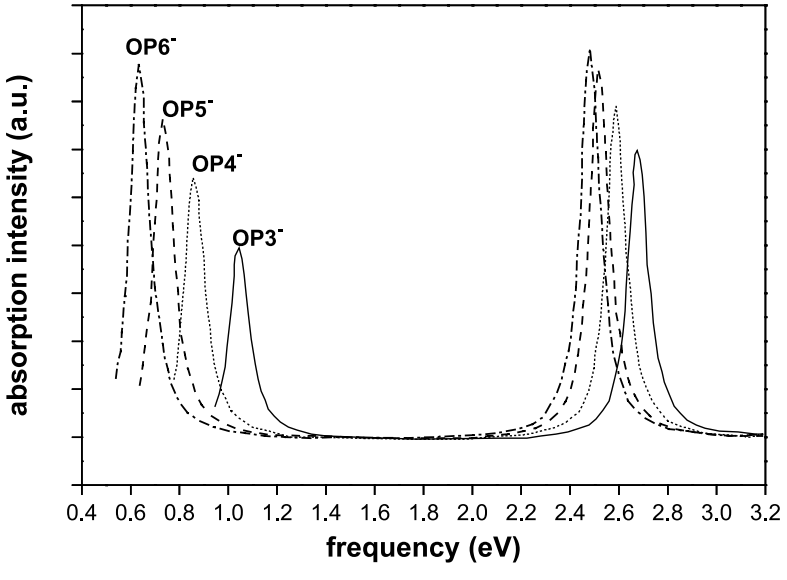

Fig. 6. EOM-CCSD/INDO calculated optical absorption spectra of an electron polaron in oligophenylenes.

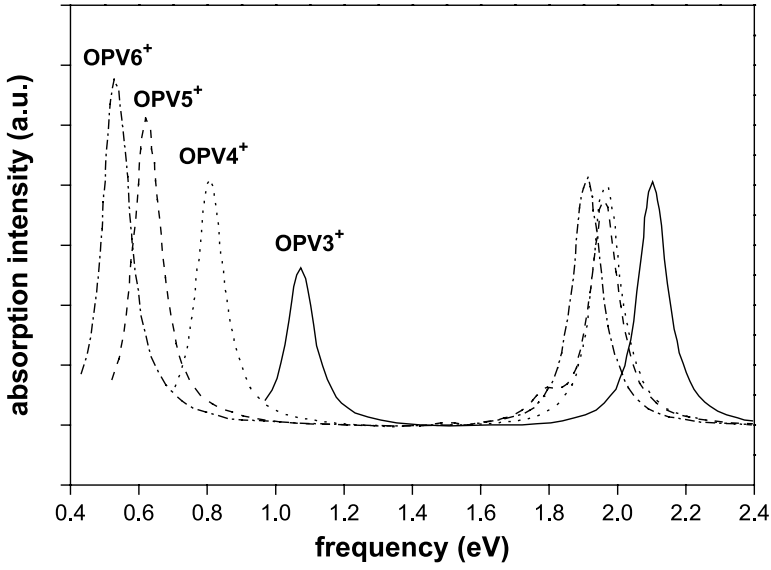

Fig. 7. EOM-CCSD/INDO calculated optical absorption spectra of a hole polaron in oligo(phenylenevinylene)s.

POL1 → POL2 transitions, see Fig. 3. This fully supports the configuration interaction analysis by Bally *et al.*[30] Then the transition moment can be simplified as:

$$\langle g\,|\mu\,|m\rangle \approx \sum_{\nu} R_{\nu}^{m}\bar{\mu}_{1\nu} \approx -R_{\mathrm{HOMO}\to\mathrm{POL1}}\bar{\mu}_{\mathrm{HOMO,POL1}} + R_{\mathrm{POL1}\to\mathrm{POL2}}\bar{\mu}_{\mathrm{POL1,POL2}}. \tag{41}$$

Thus, the relative intensities of LE with respect to HE depend on the relative signs of wavefunction R's. It is the interference effect to reduce the intensity of the LE peak. Thus, we can expect that if the polaron geometry relaxation is large, then from Fig. 3, the two sub-gap transitions are closer in energy, namely, the separation of LE and HE is larger. In this case, the quantum interference effect is more pronounced. Namely, the LE intensity becomes lower. In other word, the relative intensity of LE with respect to HE manifest the polaron relaxation. Thus, from Figs. 4 and 5, we can directly predict that in polyacetylene and polythiophene, the electron phonon interaction is large, or the polymer is really soft, which is more readily to deform upon charge injection. From Figs. 6 and 7, we observe that both PPP and PPV are relatively rigid polymer. Thus, from our EOM-CCSD analysis, we propose a practical way to quantify the "electronic rigidity" by measuring the optical absorption for polaron.

Our INDO/EOM-CCSD calculations cannot only give the above qualitative picture, but also can be compared with the experiments in a satisfactory way. For

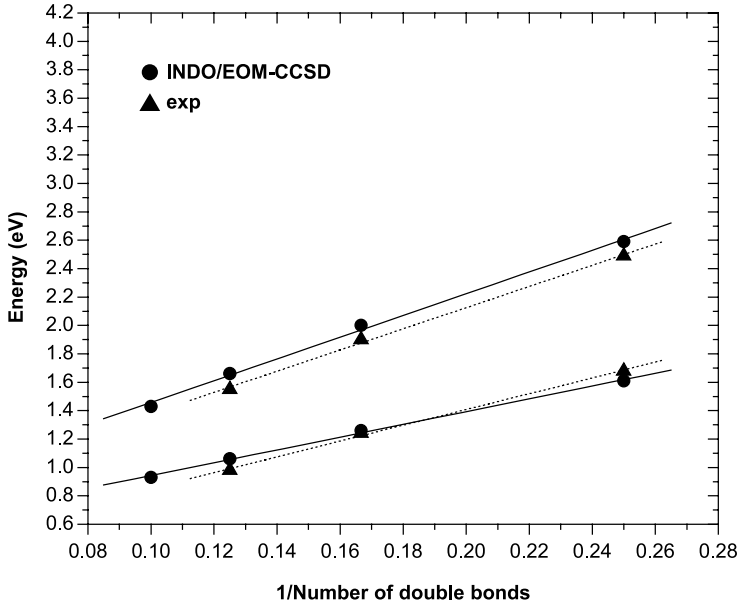

Fig. 8. Comparison of the LE and HE peak positions as calculated within the INDO/EOM-CCSD with the experimental results of Bally *et al.*[30]

example, in Fig. 8, we plot the calculated and the measured LE and HE peak positions for polyenes (measured data from Bally *et al.*[30]). The overall agreements are quite satisfactory. Our calculated LE and HE positions are also found in excellent agreement with the experiments for oligothiophene,[31] oligophenylene,[32] and oligo(phenylenevinylene)s,[33] which we will not discuss in detail here.

5. Summary

To conclude, we have presented our implementation of the semiempirical INDO coupled cluster equation of motion methods for the excited state properties. We have developed a nonlinear response theory based on it, and we have shown that nonlinear response linear equations are convergent even for near resonance region. We also implemented this approach for charge ionizing or attaching systems and apply it for calculating the optical absorption for polarons in conjugated polymers. We find that from the relative intensity of the low energy peak and the high energy peak, one can quantify whether the polymer is soft or not upon charge injections.

Acknowledgments

The authors first acknowledge the essential contributions to this short review of several collaborators: Dr. Aijun Ye, Dr. David Beljonne, and Prof. Jean-Luc Brédas.

This work is also supported by NSFC (grant Nos. 90203015, 20433070), the Ministry of Science and Technology "973 program" project No. 2002CB613406, and the CNIC supercomputer center of Chinese Academy of Sciences.

Appendix: Similarity Transformed Effective Hamiltonian

The coupled cluster effective Hamiltonian for the excited states can be evaluated as:

$$\bar{H} = \exp(-T)H\exp(T) = H + H_1 + H_2 + \frac{1}{2}H_{11} + H_{12} + \frac{1}{2}H_{22} + \frac{1}{6}H_{111} + \frac{1}{2}H_{112} + \frac{1}{24}H_{1111},$$

where H is the original Hamiltonian and the rest terms are defined as:

$$H_1 = \sum_{\substack{ai\\p}}(p^+ih_{pa} - a^+ph_{ip})t_i^a + \frac{1}{2}\sum_{\substack{ai\\pqr}}(a^+p^+qr\langle pi||rq\rangle + p^+q^+ri\langle pq||ar\rangle)t_i^a,$$

$$H_2 = \sum_{\substack{a>b\\i>j\\p}}(p^+ib^+jh_{pa} - a^+pb^+jh_{ip} + a^+ip^+jh_{pb} - a^+ib^+ph_{jp})t_{ij}^{ab}$$
$$+ \frac{1}{2}\sum_{\substack{a>b\\i>j\\pqr}}(-p^+a^+qrb^+j\langle pi||rq\rangle + p^+q^+rib^+j\langle pq||ar\rangle$$
$$- a^+ip^+b^+qr\langle pj||rq\rangle + a^+ip^+q^+rj\langle pq||br\rangle)t_{ij}^{ab},$$

$$H_{11} = \sum_{abij}(-b^+ih_{ja} - a^+jh_{ib})t_i^at_j^b + \frac{1}{2}\sum_{\substack{abij\\pq}}(p^+q^+ji\langle pq||ab\rangle + b^+a^+pq\langle ji||qp\rangle$$
$$+ 4b^+p^+qi\langle pj||aq\rangle)t_i^at_j^b,$$

$$H_{12} = \sum_{\substack{ai\\b>c,\,j>k}}(-b^+ic^+kh_{ja} - b^+jc^+ih_{ka} - a^+jc^+kh_{ib} - b^+ja^+kh_{ic})t_i^at_{jk}^{bc}$$
$$+ \frac{1}{2}\sum_{\substack{ai\\b>c,\,j>k\\pq}}(-b^+a^+pqc^+k\langle ji||qp\rangle - b^+jc^+a^+pq\langle ki||qp\rangle$$
$$+ p^+q^+jic^+k\langle pq||ab\rangle + b^+jp^+q^+ki\langle pq||ac\rangle$$
$$+ 2p^+a^+qjc^+k\langle pi||bq\rangle + 2b^+jp^+a^+qk\langle pi||cq\rangle - 2p^+b^+qic^+k\langle pj||aq\rangle$$
$$- 2b^+jp^+c^+qi\langle pk||aq\rangle)t_i^at_{jk}^{bc},$$

$$H_{22} = \frac{1}{2}\sum_{\substack{a>b,\,i>j\\c>d,\,k>l\\pq}}(c^+a^+pqb^+jd^+l\langle ki||qp\rangle + c^+kd^+a^+pqb^+j\langle li||qp\rangle$$

$$
\begin{aligned}
&+ p^+q^+kib^+jd^+l\,\langle pq|\,|ac\rangle + c^+kp^+q^+lib^+j\,\langle pq|\,|ad\rangle \\
&+ a^+ic^+b^+pqd^+l\,\langle kj|\,|qp\rangle + c^+ka^+id^+b^+pq\,\langle lj|\,|qp\rangle \\
&+ a^+ip^+q^+kjd^+l\,\langle pq|\,|bc\rangle + c^+ka^+ip^+q^+lj\,\langle pq|\,|bd\rangle \\
&- 2p^+a^+qkb^+jd^+l\,\langle pi|\,|cq\rangle - 2c^+kp^+a^+qlb^+j\,\langle pi|\,|dq\rangle \\
&- 2p^+c^+qib^+jd^+l\,\langle pk|\,|aq\rangle - 2c^+kp^+d^+qib^+j\,\langle pl|\,|aq\rangle \\
&- 2a^+ip^+b^+qkd^+l\,\langle pj|\,|cq\rangle - 2c^+ka^+ip^+b^+ql\,\langle pj|\,|dq\rangle \\
&- 2a^+ip^+c^+qjd^+l\,\langle pk|\,|bq\rangle - 2c^+ka^+ip^+d^+qj\,\langle pl|\,|bq\rangle)t_{ij}^{ab}t_{kl}^{cd},
\end{aligned}
$$

$$
H_{111} = 3\sum_{\substack{abc,\,ijk\\ p}} (b^+a^+pk\,\langle ji|\,|cp\rangle - p^+a^+kj\,\langle pi|\,|bc\rangle)t_i^at_j^bt_k^c,
$$

$$
\begin{aligned}
H_{112} = \sum_{\substack{ai,\,bj\\ c>d,\,k>l\\ p}} &(b^+a^+pkd^+l\,\langle ji|\,|cp\rangle + c^+kb^+a^+pl\,\langle ji|\,|dp\rangle \\
&- p^+c^+jid^+l\,\langle pk|\,|ab\rangle - c^+kp^+d^+ji\,\langle pl|\,|ab\rangle + 2c^+a^+pjd^+l\,\langle ki|\,|bp\rangle \\
&- 2p^+a^+kjd^+l\,\langle pi|\,|bc\rangle \\
&+ 2c^+kd^+a^+pj\,\langle li|\,|bp\rangle - 2c^+kp^+a^+lj\,\langle pi|\,|bd\rangle)t_i^at_j^bt_{kl}^{cd}, \text{ and}
\end{aligned}
$$

$$
H_{1111} = 6\sum_{\substack{abcd\\ ijkl}} b^+a^+lk\,\langle ji|\,|cd\rangle\, t_i^at_j^bt_k^ct_l^d.
$$

References

1. Shirakawa H, Louis EJ, MacDiarmid AG, Chiang CK, Heeger AJ, *Chem Commun* **578**: 1977.
2. Mele G, Epstein A (eds.), *Synth Met* **125**:1–138, 2002.
3. Longuet-Higgins HC, Salem L, *Proc Roy Soc London* **A251**:172, 1959; Fröhlich H, *Proc Roy Soc London* **A223**:296, 1954.
4. Pople JA, Walmsley SH, *Mol Phys* **5**:15, 1962.
5. Reierls RE, *Quantum Theory of Solids*, Clarendon, Oxford, pp. 108, 1955; Heeger AJ, Kivelson S, Schrieffer JR, Su WP, *Rev Mod Phys* **60**:781, 1988; Su WP, Schieffer JR, Heeger AJ, *Phys Rev Lett* **42**:1698, 1979.
6. Ovchinnikov AA, Ukrainskii II, Kventsel GV, *Sov Phys Usp* **15**:575, 1973; Tavan P, Schulten K, *J Chem Phys* **85**:6602, 1986.
7. Gammel JT, Campbell DK, Mazumdar S, Dixit SN, Loh EY, *Synth Metals* **43**:3471, 1991.
8. Brédas JL, Street GB, *Acc Chem Res* **18**:309, 1985.
9. Brédas JL, in Skotheim TA (ed.), *Handbook of Conducting Polymers*, Vol. 2, Chap. 25, Dekker, New York, pp. 859–913, 1986.
10. André JM, Delhalle J, Brédas JL, *Quantum Chemistry Aided Design of Organic Polymers. An Introduction to the Quantum Chemistry of Polymers and its Applications*, World Scientific, Singapore, 1991.
11. Hudson BS, Kohler BE, Schulten K, in Lim EC (ed.), *Excited States*, Academy Press, pp. 1–95, 1982.

12. Beljonne D, Shuai Z, Serrano-Andrés L, Brédas JL, *Chem Phys Lett* **279**:1, 1997.
13. Runge E, Gross EKU, *Phys Rev Lett* **52**:997, 1984.
14. Yokojima S, Chen GH, *Chem Phys Lett* **355**:400, 2002.
15. Tavan P, Schulten K, *Phys Rev B* **36**:4337, 1987; Soos ZG, Ramasesha S, Galvão DS, *Phys Rev Lett* **71**:1609, 1993.
16. White SR, *Phys Rev Lett* **69**:2863, 1992; Shuai Z, Brédas JL, Su WP, Pati SK, Ramasesha S, *Phys Rev B* **55**:15368, 1997; Shuai Z, Brédas JL, Pati SK, Ramasesha S, *Phys Rev B* **58**:15329, 1998.
17. Shuai Z, Brédas JL, *Phys Rev B* **62**:15452, 2000.
18. Ye A, Shuai Z, Kwon O, Brédas JL, Beljonne D, *J Chem Phys* **121**:5567, 2004.
19. Bartlett RJ, *Ann Rev Phys Chem* **32**:359, 1981; Cizek J, Paldus J, *Phys Scr* **21**:251, 1980; Stanton JF, Bartlett RJ, *J Chem Phys* **98**:7029, 1993.
20. Scheiner AC, Scuseria GE, Rice JE, Lee TJ, Schaefer HF, *J Chem Phys* **87**:5361, 1987.
21. Guo D, Mazumdar S, Dixit SN, Kajzar F, Jarka F, Kawabe Y, Peyghambarian N, *Phys Rev* **B48**:1433, 1993.
22. Yaron D, Moore EE, Shuai Z, Brédas JL, *J Chem Phys* **108**:7451, 1998.
23. Orr BJ, Ward JF, *Mol Phys* **20**:513, 1971.
24. Shuai Z, Ramasesha S, Brédas JL, *Chem Phys Lett* **250**:14, 1996; Ramasesha S, Shuai Z, Brédas JL, *Chem Phys Lett* **245**:224, 1995; Wang WZ, Shuai Z, Saxena A, Bishop AR, Brédas JL, *Phys Rev B* **59**:1697, 1999; Pati SK, Ramasesha S, Shuai Z, Brédas JL, *Phys Rev B* **59**:14827, 1999.
25. Shuai Z, Brédas JL, Sexena A, Bishop AR, *J Chem Phys* **109**:2549, 1998.
26. Zhu L, Yang X, Yi Y, Xuan P, Shuai Z, Chen D, Zojer E, Brédas JL, Beljonne D, *J Chem Phys*, December 1, 2004.
27. Wintgen V, Valat P, Garnier F, *J Phys Chem* **98**:228, 1994.
28. Fesser K, Bishop AR, Campbell DK, *Phys Rev B* **27**:4804, 1983.
29. Burroughes JH *et al.*, *Nature (London)* **347**:539, 1990; Gustafsson G *et al.*, *Nature (London)* **357**:477, 1992; Friend RH *et al.*, *Nature* **397**:121, 1999.
30. Bally T, Roth K, Tang W, Schrock RR, Knoll K, Park LY, *J Am Chem Soc* **114**:2440, 1992.
31. Apperloo JJ, Groenendaal L, Verheyen H *et al.*, *Chem Eur J* **8**:2384, 2002.
32. Khanna RK, Jiang YM, Srinivas B, Smithhart CB, Wertz DL, *Chem Mater* **5**:1792, 1993.
33. Schenk R, Gregorius H, Müllen K, *Adv Mater* **3**:492, 1991.